JACS
JOURNAL OF THE AMERICAN CHEMICAL SOCIETY
Communication
pubs.acs.org/JACS

Electron Microscopic Observation of Selective Excitation of Conformational Change of a Single Organic Molecule

Ricardo M. Gorgoll,[†] Emrah Yücelen,[‡] Akihito Kumamoto,[§] Naoya Shibata,[§] Koji Harano,*[,†] and Eiichi Nakamura*[,†,∥]

[†]Department of Chemistry, The University of Tokyo, 7-3-1 Hongo, Bunkyo-ku, Tokyo 113-0033, Japan

[‡]FEI Company, Europe NanoPort, Achtseweg Noord 5, 5651 GG Eindhoven, The Netherlands

[§]Institute of Engineering Innovation, Graduate School of Engineering, The University of Tokyo, 2-11-16 Yayoi, Bunkyo-ku, Tokyo 113-8656, Japan

[∥]CREST, JST, 7-3-1 Hongo, Bunkyo-ku, Tokyo 113-0033, Japan

Supporting Information

ABSTRACT: Atomic resolution transmission electron microscopic observations at different electron acceleration voltages enabled us to observe visually the energy relaxation process of one conformer into another via rotation of various parts of the molecule. Cross-correlation analysis of sequential transmission electron microscopy (TEM) images or of the difference between experimental and simulated TEM images has been utilized for investigation of the conformational mobility and for structure identification of conformers.

Although σ-bond rotation and the ensuing conformational changes are the fundamental subject of chemistry,[1,2] the possibility of visually observing such events at atomic resolution has long eluded the ability of chemists.[3,4] We recently tested the utility of transmission electron microscopy (TEM)[5,6] and acquired in situ atomic resolution movies of the conformational changes of single organic molecules attached to the surface of a carbon nanohorn (CNH, a tapered variant of a single-walled carbon nanotube).[7−9] However visually impressive, the movies themselves are insufficient as a research tool in the absence of a method to change and quantify the magnitude and frequency of the motions. The molecular motions under study were found to be unusually insensitive to temperature and do not follow the Arrhenius equation (between 4[10] and 793 K[11]), and therefore, the standard temperature probe cannot be used. We report here that the frequency of the molecular motions can be increased by lowering the electron accelerating voltage (from 120 to 80 to 60 kV) as a consequence of large scattering cross section[12] and that the motions can be quantified using cross-correlation analysis[13,14] between the neighboring frames of the movie. Cross-correlation analysis has been shown to be useful for computer-aided structural identification of the conformer seen in each frame of the molecular movie. As a platform for this study, we examined biotin derivatives **1** and **2** attached to the surface of a CNH through two different linkers (Figure 1a) whose motions were observed as they happened during several minutes on a TEM stage at the three different voltages (Figure 1b). We call this imaging method single-molecule and real-time TEM (SMART-TEM) imaging. Molecule **1** is rather static at 80 and 120 kV, but vibrates frequently at 60 kV (Figure 1b). In contrast, the more flexible molecule **2** is mobile enough at 80 kV to show us visually the process of stepwise energy relaxation by sequential rotations of σ-bonds in vacuum (Figure 1a), a piece of information so far unobtainable by experimental methods but only by theoretical simulations.[15−17]

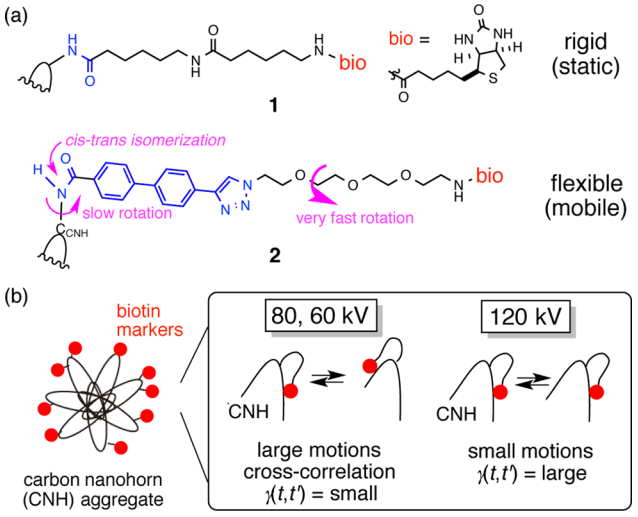

Figure 1. Biotinylated molecules **1** and **2** on CNH. (a) Molecular designs. (b) Molecular motions faster and cross correlation smaller at 60 and 80 kV than those at 120 kV under SMART-TEM conditions.

Molecules **1** and **2** are designed to differ in their flexibility (Figure 1a). They have in common a biotin terminus connected to the CNH via a linker of different flexibility. Molecule **1** has a rather inflexible tripeptide linker that makes the molecule rather static under 120 kV SMART-TEM conditions.[18] Molecule **2** consists of three different rotating parts, a frequently rotating oligoethyleneoxy (OEO) linker, a less flexible N−C_{CNH} bond, and the least rotating N−C(=O) bond. Therefore, the conformational changes of each part of **2** will occur on three different time scales. The CNH aggregates bearing a number of specimen molecules were placed on a TEM sample stage at 298

Received: January 16, 2015
Published: March 3, 2015

DOI: 10.1021/jacs.5b00511
J. Am. Chem. Soc. 2015, 137, 3474−3477

K, irradiated at an electron dose rate of 10^4–10^6 e^- nm^{-2} s^{-1}, and the SMART-TEM movie was acquired for ca. 1 min for each molecule.

For 27 molecules carefully analyzed here during our typical observation period of a few minutes or a few hundred frames (electron dose of $<10^8$ e^- nm^{-2}), we did not find total loss of the molecules, fragmentation, or rearrangement that would occur by radiolysis or knock-on damage. This observation agrees with our previous finding that single molecules under the SMART-TEM conditions retain their structurally integrity, in contrast to the same molecule in its solid state that decomposed immediately under irradiation at the same dose rate.[8]

The motions of **1**, both at 120 kV (Figure 2a)[18] and at 80 kV (Figure 2b) were found to be equally slow, as seen for the biotin terminal (red arrow) touching the same area of the CNH surface even after 47–50 s. At 60 kV (Figure 2c), however, the frequency and magnitude of the conformational changes became much larger, as shown by the motion of the biotin group (red arrows) over a distance of ca. 2.2 nm around the CNH surface. We noticed that the 60 kV acceleration voltage (i.e., longer wavelength) reduces the image resolution. As shown in the 100 consecutive frames taken during 40 s at 80 kV (Figure 2d), molecule **2** underwent much larger conformational changes than molecule **1** under the same voltage (Figure 2b).

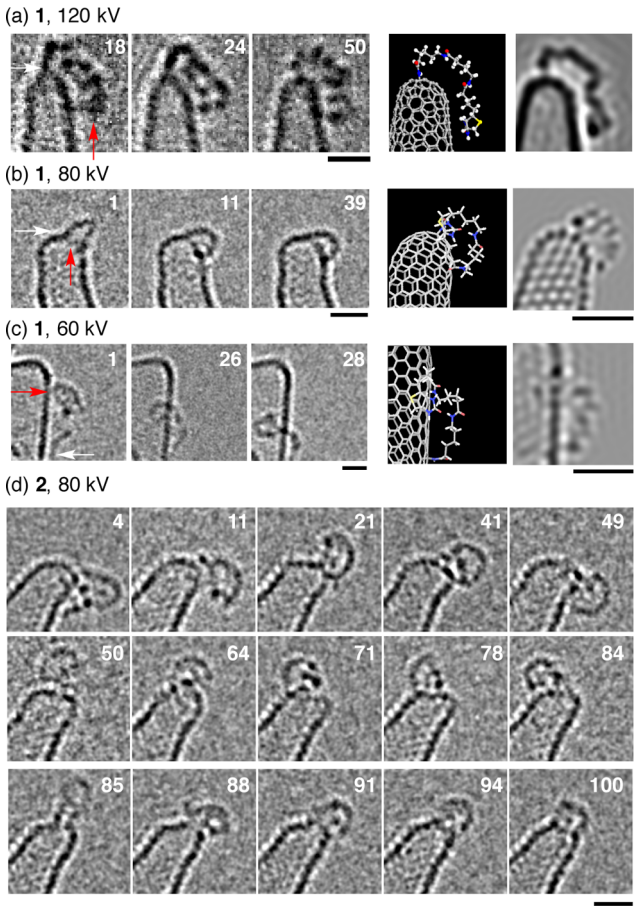

Figure 2. Representative images of molecules **1** and **2** extracted from TEM movies at different acceleration voltages. A plausible molecular model and its simulated TEM image are shown for molecule **1**. The number refers to the frame number sequentially numbered from the beginning of the imaging. The red arrow points to the biotin terminal and the white arrow to the amide group connected to the CNH. Scale bars are 1 nm. (a) Molecule **1** is seen to be rather static at 120 kV. Irradiated for 50 s with a total dose of 3.0×10^6 e^- nm^{-2}. Images are adapted from ref 18. Copyright 2008 American Chemical Society. (b) Molecule **1** is seen to be static at 80 kV. Irradiated for 47 s with a total electron dose of 6.1×10^7 e^- nm^{-2}. (c) Rapidly moving **1** at 60 kV. Irradiated for 12 s with a total electron dose of 3.6×10^5 e^- nm^{-2}. (d) Rapidly moving **2** at 80 kV. Irradiated for 40 s with a total electron dose of 1.0×10^8 e^- nm^{-2}. Simulation images were generated by a multislice procedure implemented using standard simulation software.[19] The original TEM movies can be found in the Supporting Information.

To quantify the visual image analysis in the above paragraph, we quantified the image changes using cross-correlation image analysis.[20,21] The cross-correlation factor between two consecutive frames at times t and t', $\gamma(t,t')$ in eq 1, was calculated, where $I_t(r_{ij})$ and $I_{t'}(r_{ij})$ are the intensities of pixel (ij) in frames t and t', and $\overline{I}_t$ and $\overline{I}_{t'}$ are the mean of $I_t(r_{ij})$ and $I_{t'}(r_{ij})$. This value represents the degree of matching between the two neighboring frames as a number (absolute value) between 1 and 0, 1 being a perfect match and 0 being no match (cf. Figure 1b). Thus, the sudden drop of the γ value often seen in Figure 3a corresponds to a big conformational change followed by small conformational changes.

$$\gamma(t, t') = \frac{\sum_{ij}^{N} [I_t(r_{ij}) - \overline{I}_t]\cdot[I_{t'}(r_{ij}) - \overline{I}_{t'}]}{\sqrt{\sum_{ij}^{N} [I_t(r_{ij}) - \overline{I}_t]^2}\cdot\sqrt{\sum_{ij}^{N} [I_{t'}(r_{ij}) - \overline{I}_{t'}]^2}} \quad (1)$$

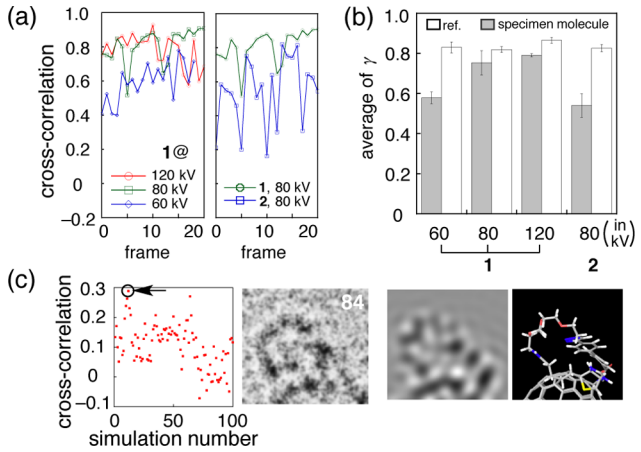

Figure 3. Cross-correlation analysis of the images in the SMART-TEM movies of **1** and **2**. (a) Cross correlation, γ, calculated from consecutive frames of the movie of **1** at 60–120 kV (left) and **1** and **2** at 80 kV (right). (b) Average of γ for **1** and **2** at different voltages with standard error bars calculated for three specimen molecules. The values for CNH images are shown as a reference. (c) An example of cross-correlation analysis for comparison between the image in frame 84 and 100 images generated by the OPLS-2005-based MD simulation of **2** (left). The simulated image that has the highest correlation (circle and arrow) is shown on the right together with the corresponding molecular model.

The average cross-correlation values (Figure 3a, left box) in the movie of one molecule of **1** were 0.58 ± 0.03 at 60 kV (blue line), 0.75 ± 0.06 at 80 kV (green), and 0.79 ± 0.01 at 120 kV (red) (Figure 3b, left half), suggesting that there is a threshold between 60 kV and 80–120 kV. This threshold is because of the energy barrier for conformational changes as discussed below. Note that the reference γ values calculated for the CNH substrate depend neither on the acceleration voltage nor on the molecules, as one expects (Figure 3b, reference values, white bars).

DOI: 10.1021/jacs.5b00511
J. Am. Chem. Soc. 2015, 137, 3474–3477

The right-hand box of Figure 3a shows the γ values for 20 consecutive frames of a movie taken for single molecules of **1** and **2** at 80 kV. Here, not only is the γ value consistently smaller for **2** than for **1** (i.e., continuous small motions) but also a large drop of the value (large motions) occurs more frequently. The averaged data are summarized in the right half of Figure 3b: **1** (0.75 ± 0.06) and **2** (0.68 ± 0.02). The data confirm our visual analysis that **2** is more mobile at the same voltage of 80 kV.

Cross-correlation analysis is useful for quick comparisons between experimental and numerous molecular dynamics (MD) images, as shown in Figure 3c: frame 84 is compared with 100 simulated images of the conformers generated by MD, where we find that the one circled in the graph shows the best fit. A more detailed computational structural search may be carried out based on this conformer.

To gain deeper understanding of the observed mobility of **2**, we investigated 100 consecutive SMART-TEM images (see the Supporting Information; partly shown in Figure 2d) by comparison with images obtained through MD using the OPLS-2005 force field[22] for a temperature and time range of 100−1000 K and 1 ns to microseconds (μs) (see Supporting Information for details). In Figure 2d, we see two conformational changes just after frames 49 and 84 that separate the whole scene into three phases. In the first phase, frames 1 to 49, the molecule is mainly located on the right-hand side of the CNH (Figure 2d, top row). In the second phase, frames 50 to 84, the molecule is located on the left-hand side of the CNH (Figure 2d, middle). In the last phase, the molecule becomes perpendicular to the CNH cap at frame 85 and then is mainly located above the cap region (Figure 2d, bottom). In each phase, smaller conformational changes also occurred at every frame. The dynamic profile found here is in agreement with the molecular design of **2**, where the motions are expected to occur on three different time scales. The structures of the three typical conformers are shown in Figure 4 (see Supporting Information for some additional conformers). The bicyclic biotin terminal (red circle in models) appears as one of the dark spots, serving hence as a marker. We therefore conclude that the major conformational changes are due to rotation of the OEO group, the N−C_{CNH} bond (dihedral angle θ^1 in Figure 5a), and the N−C(O) bond (θ^2).

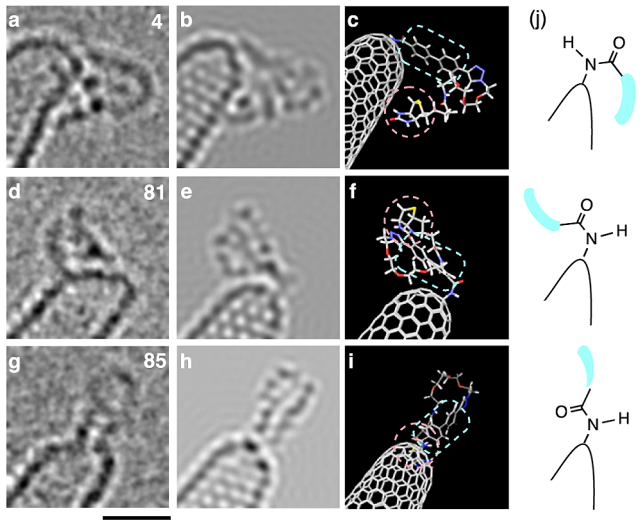

Figure 4. Plausible conformations of frames 4, 81, and 85 of a TEM movie of **2** at 80 kV. Orange circle = biotin terminus. Blue square = biphenyl. (a−i) The TEM image is shown on the left, a molecular model of a plausible conformation is shown on the right, and its TEM simulation is shown in the middle. Scale bar is 1 nm. (j) Schematic image of the conformational changes of **2** showing the biphenyl/OEO group in blue.

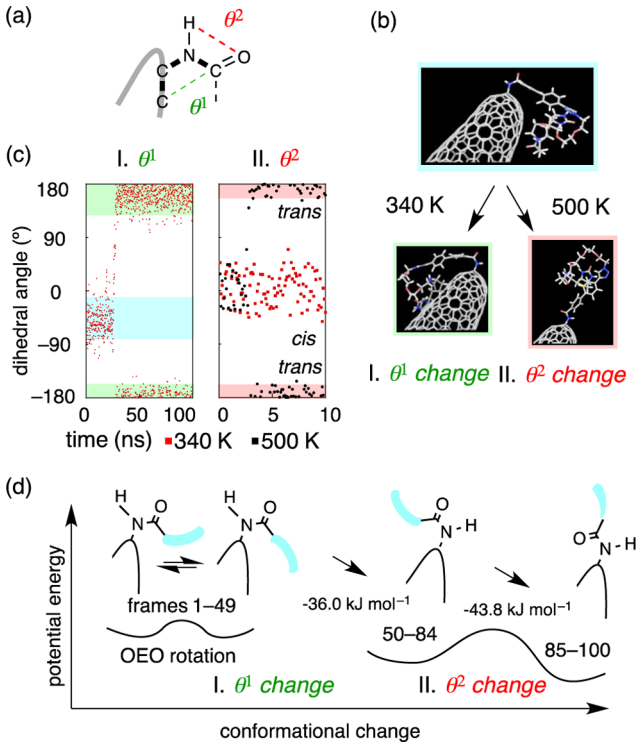

Figure 5. MD simulation of **2**. (a) The two dihedral angle changes, θ^1 and θ^2. (b) Molecular models of **2** after simulation runs at 340 and 500 K. (c) Time evolution of dihedral angles θ^1 and θ^2. The blue, green, and red color codes correspond to those in panel b. (d) An approximate potential surface for the conformational change of **2** as deduced from the time evolution of the TEM images supported by the MD calculations.

Next, we describe the origin of the observed conformational changes and energetics based on molecular dynamics simulations illustrated for three runs in Figure 5c. Starting with the conformer seen in frame 4 (Figure 4c) as the initial state at 340 K for 100 ns, we see the first big conformational change occurring after frame 49 (Figure 5bI; blue frame to green). We needed 500 K to simulate the conformational changes shown in frames 85−100 that occurred on a room temperature sample stage for a period of a minute (Figure 5bII, blue to red). The slow motion under SMART-TEM conditions is reminiscent of scanning tunneling microscope conditions where a specimen molecule is fixed on a macroscopic substrate and hardly vibrates or translates.

The conformational change seen after frame 49 is due to the rotation of the N−C_{CNH} bond (θ^1 in Figure 5a). Up to 28 ns in the simulation at 340 K (Figure 5c left), θ^1 remains largely in the range −20 to −80° (blue band), then suddenly and irreversibly increases thereafter to 150−180° and −170 to −180° (green band) with an average potential energy decrease of 36.0 kJ mol^{-1} because of the N−C_{CNH} bond rotation. Here, the numerous conformers with slightly different θ values have the OEO groups in different conformations. The conformers differ from each other by approximately 30 kJ mol^{-1} in energy.

The big conformational change just after frame 84 in Figure 2d is because of the change in θ^2, i.e., cis to trans isomerization of the amide bond that took place in the simulation at 500 K, as

DOI: 10.1021/jacs.5b00511
J. Am. Chem. Soc. 2015, 137, 3474−3477

illustrated in the run shown in Figure 5cII in black dots. This process accompanies an average energy decrease of 43.8 kJ mol^{-1}. At 340 K, θ^2 does not change, as shown by the red dots. Obviously, the cis to trans isomerization of the amide bond requires a higher activation energy (500 K) than the N−C_{CNH} bond rotation (340 K).

The approximate energetics obtained by the molecular dynamics calculations for the images shown in Figure 2d are summarized in Figure 5d. The group of conformers seen in frames 1−49 is the least stable group, which involves a *cis*-amide, a small θ^1 value, and a variety of OEO conformations. The N−C_{CNH} bond rotation (θ^1) results in the more stable conformers seen in frames 50−84, and the cis-to-trans amide rotation (θ^2) results in the most stable conformers seen in frames 85−100.

In conclusion, we have visually observed the time evolution of the conformational changes of two types of molecules **1** and **2** by SMART-TEM imaging and found that the magnitude of the acceleration voltage affects the frequency of conformational changes, as analyzed by cross-correlation analysis of the consecutive images. The motion was found to become more frequent as the voltage was lowered from 120 to 60 kV. Though this observation may be counterintuitive at first glance, it agrees with the larger scattering cross section in vacuum between a slower electron and the nuclei in the specimen molecule.[12] The two new tools, voltage control and cross-correlation image analysis introduced here, will enhance the utility of SMART-TEM imaging in the analysis of systems involving complex structural changes and chemical reactions.[23−28]

■ ASSOCIATED CONTENT

Ⓢ Supporting Information

Sample preparation, TEM conditions, and simulations. This material is available free of charge via the Internet at http://pubs.acs.org.

■ AUTHOR INFORMATION

Corresponding Authors

*harano@chem.s.u-tokyo.ac.jp

*nakamura@chem.s.u-tokyo.ac.jp

Notes

The authors declare no competing financial interest.

■ ACKNOWLEDGMENTS

We acknowledge Prof. Yuichi Ikuhara of the Institute of Engineering Innovation, School of Engineering, for useful comments on TEM images. We thank Mr. Akira Yasuhara (JEOL Ltd.) for TEM measurements at 60 kV. This research is supported by KAKENHI (No. 26708016 to K.H.), MEXT, Japan. A part of this work was conducted in Research Hub for Advanced Nano Characterization, The University of Tokyo, and a part of this work was supported by "Nanotechnology Platform" (project No. 12024046) both sponsored by MEXT, Japan. R.M.G. thanks JSPS for a predoctoral fellowship.

■ REFERENCES

(1) (a) Sachse, H. *Ber. Dtsch. Chem. Ges.* **1890**, *23*, 1363−1370. (b) Burkert, U.; Allinger, N. L. *Molecular Mechanics*; American Chemical Society: Washington, D.C., 1982.

(2) Eliel, E. L.; Wilen, S. H. *Stereochemistry of Organic Compounds*; Wiley-Interscience: New York, 1994.

(3) Karplus, M.; McCammon, A. *Nat. Struct. Biol.* **2002**, *9*, 646−652.

(4) Bande, A.; Michl, J. *Chem.−Eur. J.* **2009**, *15*, 8504−8517.

(5) Koshino, M.; Tanaka, T.; Solin, N.; Suenaga, K.; Isobe, H.; Nakamura, E. *Science* **2007**, *316*, 853.

(6) Nakamura, E. *Angew. Chem., Int. Ed.* **2013**, *52*, 236−252.

(7) Iijima, S.; Yudasaka, M.; Yamada, R.; Bandow, S.; Suenaga, K.; Kokai, F.; Takahashi, K. *Chem. Phys. Lett.* **1999**, *309*, 165−170.

(8) Harano, K.; Takenaga, S.; Okada, S.; Niimi, Y.; Yoshikai, N.; Isobe, H.; Suenaga, K.; Kataura, H.; Koshino, M.; Nakamura, E. *J. Am. Chem. Soc.* **2014**, *136*, 466−473.

(9) Harano, K.; Homma, T.; Niimi, Y.; Koshino, M.; Suenaga, K.; Leibler, L.; Nakamura, E. *Nat. Mater.* **2012**, *11*, 877−881.

(10) Koshino, M.; Solin, N.; Tanaka, T.; Isobe, H.; Nakamura, E. *Nat. Nanotechnol.* **2008**, *3*, 595−597.

(11) Koshino, K.; Niimi, Y.; Nakamura, E.; Kataura, H.; Okazaki, T.; Suenaga, K.; Iijima, S. *Nat. Chem.* **2010**, *2*, 117−124.

(12) Williams, D. B.; Carter, C. B. *Transmission Electron Microscopy: A Textbook For Materials Science*, 2nd ed.; Springer Science + Business Media LLC: New York, 2009.

(13) Frank, J. In *Computer Processing of Electron Microscope Images*; Hawkes, P. W., Ed.; Springer: Berlin, Germany, 1980; p 187.

(14) Mobus, G.; Schweinfest, R.; Gemming, T.; Wagner, T.; Ruhle, M. *J. Microsc.* **1998**, *190*, 109.

(15) Tasis, D.; Tagmatarchis, N.; Bianco, A.; Prato, M. *Chem. Rev.* **2006**, *106*, 1105.

(16) Garg, A.; Sinnott, S. B. *Chem. Phys. Lett.* **1998**, *295*, 273.

(17) Johnson, R. R.; Johnson, A. T. C.; Klein, M. L. *Nano Lett.* **2008**, *8*, 69.

(18) Nakamura, E.; Koshino, M.; Tanaka, T.; Niimi, Y.; Harano, K.; Nakamura, Y.; Isobe, H. *J. Am. Chem. Soc.* **2008**, *130*, 7808−7809.

(19) Kirkland, E. J. *Advanced Computing in Electron Microscopy*; Plenum: London, 1998.

(20) Du, K.; von Hochmeister, K.; Phillipp, F. *Ultramicroscopy* **2007**, *107*, 281.

(21) Barwick, B.; Park, H. S.; Kwon, O.-H.; Baskin, J. S.; Zewail, A. H. *Science* **2008**, *322*, 1227−1231.

(22) Banks, J. L.; Beard, H. S.; Cao, Y.; Cho, A. E.; Damm, W.; Farid, R.; Felts, A. K.; Halgren, T. A.; Mainz, D. T.; Maple, J. R.; Murphy, R.; Philipp, D. M.; Repasky, M. P.; Zhang, L. Y.; Berne, B. J.; Friesner, R. A.; Gallicchio, E.; Levy, R. M. *J. Comput. Chem.* **2005**, *26*, 1752.

(23) Hashimoto, A.; Yorimitsu, H.; Ajima, K.; Suenaga, K.; Isobe, H.; Miyawaki, J.; Yudasaka, M.; Iijima, S.; Nakamura, E. *Proc. Natl. Acad. Sci. U.S.A.* **2004**, *101*, 8527−8530.

(24) Chamberlain, T. W.; Meyer, J. C.; Biskupek, J.; Leschner, J.; Santana, A.; Besley, N. A.; Bichoutskaia, E.; Kaiser, U.; Khlobystov, A. N. *Nat. Chem.* **2011**, *3*, 732−737.

(25) Schäffel, F.; Wilson, M.; Warner, J. H. *ACS Nano* **2011**, *5*, 9428.

(26) Senga, R.; Komsa, H.-P.; Liu, Z.; Hirose-Takai, K.; Krasheninnikov, A. V.; Suenaga, K. *Nat. Mater.* **2014**, *13*, 1050−1054.

(27) Li, Z. Y.; Young, N. P.; Vece, M. D.; Palomba, S.; Palmer, R. E.; Bleloch, A. L.; Curley, B. C.; Johnston, R. L.; Jiang, J.; Yuan, J. *Nature* **2008**, *451*, 46−48.

(28) Nakamura, E.; Koshino, M.; Saito, T.; Niimi, Y.; Suenaga, K.; Matsuo, Y. *J. Am. Chem. Soc.* **2011**, *133*, 14151−14153.

DOI: 10.1021/jacs.5b00511
J. Am. Chem. Soc. 2015, 137, 3474−3477